



ISSN: 0975-833X

## RESEARCH ARTICLE

### PERFORMANCE EVALUATION OF ZIRCONIUM PHOSPHATE INCORPORATED NOVEL POLYMER ELECTROLYTE MEMBRANE FOR FUEL CELLS

Perumal Bhavani, Dharmalingam Sangeetha\*

Department of Chemistry, Anna University, Chennai 600 025, India

#### ARTICLE INFO

##### Article History:

Received 07<sup>th</sup> November, 2011  
Received in revised form  
12<sup>th</sup> December, 2011  
Accepted 19<sup>th</sup> January, 2011  
Published online 29<sup>th</sup> February, 2012

##### Key words:

Zirconium phosphate; Electrolyte membrane; Proton exchange membrane;  
Fuel cell;  
SPSEBS

#### ABSTRACT

A novel composite electrolyte membrane, composed of sulfonated poly styrene ethylene butylenes poly styrene (SPSEBS) and zirconium phosphate ( $ZrPO_4$ ), was fabricated for fuel cell applications. Zirconium phosphate was prepared in-house by the reaction of zirconium oxychloride with phosphoric acid. It possesses appreciable proton conducting and donating characteristics along with excellent thermal stability and compatibility with the polymer membrane. In the fabrication of membranes, SPSEBS and  $ZrPO_4$  in tetrahydrofuran was thoroughly mixed and subsequently solvent evaporated. They were characterized by XRD, FTIR, TGA, DSC and UTM (Universal testing machine). Their ion-exchange capacity and water uptake increased with the increase in the content of  $ZrPO_4$ , but the methanol cross-over favourably reduced. The proton conductivity was in the order of  $10^{-2}$  S/cm which is an excellent result for application in fuel cells. The dispersion of  $ZrPO_4$  in the polymer matrix was uniform as evidenced by the SEM images. The fuel cell performance of the composite membranes was tested using 25 cm<sup>2</sup> cell unit.

Copy Right, IJCR, 2012, Academic Journals. All rights reserved.

#### INTRODUCTION

Proton exchange membrane fuel cells (PEMFC) are considered as the ideal sources of power for the next generation of automation, as they are claimed to be the power generators for zero-emission vehicles. Nafion membrane, a perfluorinated polymer, has been the only most efficient membrane for the use as an electrolyte in such fuel cells due to its high proton conductivity, chemical and mechanical stability [1-3]. However, the high price of Nafion [4] and the environmental hazards associated with its disposal have led to search for low-cost non-perfluorinated ionomer membranes, which are more environmentally friendly. Some of the polymer electrolyte membranes, poly ether ether ketone (PEEK) [5-7], poly (arylene-ether-sulfone) (PSU) [8-10] PVDF-graft styrene [11-13], acid doped polybenzimidazole (PBI) [14-15] and poly phosphazone [16,17] were evaluated as alternatives to Nafion membrane for application. Among them poly styrene ethylene butylene polystyrene (PSEBS) is promising since it possesses good conductivity and flexibility. PSEBS can be converted to sulfonated poly styrene ethylene butylene polystyrene (SPSEBS), a proton conducting polymer, by electrophilic substitution of the sulfonic acid groups in the polymer back, but its reduced mechanical property was a drawback. In order to improve the mechanical properties as well as to enhance the proton conductivity SPSEBS was incorporated with zirconium phosphate. Water insoluble zirconium phosphate was added to suppress crack formation due to the shrinkage caused during drying. It also contributes to conduction of protons from the phosphate moiety and crystalline water thereby reducing the humidity influence on

conductivity [18]. In this study, we successfully introduced, the solid proton conductor,  $ZrPO_4$  into the SPSEBS matrix by solvent evaporation. The results of membrane preparation, its characterization and fuel cell performance are discussed in this communication.

#### EXPERIMENTAL METHODS

##### Material

Polystyrene-block poly (ethylene butylene)-block-polystyrene (PSEBS,  $M_w = 89,000$ ) was purchased from Aldrich. Chlorosulphonic acid (CSA) was purchased from Lancaster. Tributylphosphate (TBP), phosphoric acid and zirconium oxychloride were sourced from Spectrochem, India, while hydrogen peroxide, potassium chloride and sodium carbonate were sourced from Merck. Phenolphthalein, methanol, tetrahydrofuran (THF) and chloroform were obtained from SRL.

##### Sulfonation of PSEBS

PSEBS was sulfonated as reported in the literature [19]. The Sulfonation procedure in brief is as follows. A weighed amount of polymer was dissolved in chloroform. The required amounts of TBP followed by CSA were added drop wise to the polymer solution with continuous stirring under nitrogen atmosphere. After 3 h, the reaction was terminated using methanol. The obtained ionomer was washed with water several times until the pH attained neutrality. It was then dried at 75 °C overnight. The obtained material was designated as SPSEBS.

\*Corresponding author: [sangeetha@annauniv.edu](mailto:sangeetha@annauniv.edu)

### Preparation of zirconium phosphate ( $ZrPO_4$ )

Zirconium phosphate was prepared by slowly adding 1M aqueous solution of zirconium oxy chloride to 1M Phosphoric acid the volume of which was 10 times that of zirconium oxy chloride. The precipitate was washed several times with de-ionized water, dried for 2 h at 75°C and 100% relative humidity (RH).

### Fabrication of composite membrane

The composite membranes were prepared by solvent evaporation method. First, weighed amount of SPSEBS was dissolved in THF solvent while a weight percentage of  $ZrPO_4$  was dispersed in THF. The dispersed  $ZrPO_4$  was mixed with the polymer solution which was then stirred continuously to obtain a homogeneous solution. After several hours, it was poured on to a clean glass plate and the solvent was allowed to evaporate slowly to obtain the membranes. Composite membranes were prepared with different weight percentages of  $ZrPO_4$ . All the prepared membranes were treated with 3%  $H_2O_2$  for 8 h followed by 10%  $H_2SO_4$  and finally washed with boiling water for 10 to 25 minutes.

### Ion exchange capacity, water and methanol uptake

Ion exchange capacity (IEC) depends on the number of sulphonic acid groups that are bonded to the membrane. The SPSEBS composite membrane was immersed in a saturated potassium chloride solution overnight to allow the exchange of protons with  $K^+$  ions. The protons released from the membrane were neutralized by 0.01N sodium carbonate solution. Phenolphthalein was used as the indicator. The IEC was calculated using the following formula:

$$IEC = \frac{\text{Normality of sodium carbonate} \times \text{volume of sodium carbonate}}{\text{Weight of dry membrane}} \text{ meq/g}$$

Water and methanol uptake was determined gravimetrically. Previously dried membranes were immersed in respective solvents at room temperature. Percentage uptake was calculated by using the formula:

$$\text{Percentage uptake} = \frac{\text{Wet M} - \text{Dry M}}{\text{Dry M}} \times 100$$

Where, Wet M – Weight of wet membrane (g)  
Dry M – Weight of dry membrane (g)

The stability of membranes was examined by immersing them in freshly prepared Fenton's reagent at 80 °C for duration of 8 hours. The mixture was stirred with a glass rod every 10 minutes. The stability of the membranes was determined by analysing the chemical disintegration of the membranes.

### Methanol permeability

The experiment to evaluate methanol permeability was carried out using a testing cell consisting of two reservoirs separated by an electrolyte membrane having a dense layer of either SPSEBS or composite membranes to simulate the methanol crossover setup in direct methanol fuel cell DMFC system. A two compartment glass cell was used in this experiment. The PEM was sandwiched between the donor (Chamber A) and the

receptor (Chamber B) compartments. Initially, the donor compartment was filled with 50 ml of aqueous 2M methanol solution and the receptor compartment with 50 ml of deionised water. The solution in each compartment was stirred using magnetic stirrer during measurement to maintain uniform concentration. Due to the presence of water on either side of the cell, the membrane remained hydrated. Equal amount of solution in both the compartments ensured that equal hydrostatic pressure was maintained. The change in concentration of methanol in the receptor compartment was measured as a function of time. After every one hour, few drops of solution from the receptor compartment was withdrawn by syringe and placed in a prism of the digital pocket refractometer (Atago). The permeability was determined from refractometer readings as the readings directly gives the percentage of methanol present in the solution. The methanol permeability experiments were carried out at room temperature (~30 °C) and was calculated by plotting methanol concentration in receptor compartment ( $C_B$ ) as a function of time using the following formula,

$$C_B = (AP/V_B L) C_A(t) \text{ and} \\ P = m \times (V_B/AC_A)$$

Where 'm' is the slope of the linear plot of  $C_B$  versus time, 'P' is the methanol permeability ( $cm^2/s$ ), 'A' is the membrane area ( $cm^2$ ),  $V_B$  is the volume of compartment 'B' (ml), 'L' is the film thickness (cm),  $C_A$  and  $C_B$  are the concentrations of methanol (mol) in Cell A and Cell B and 't' is time (s). A, L and  $V_B$  are the area of membrane, thickness of membrane and volume of Cell B respectively. D and K are the methanol diffusivity and partition coefficient between the membrane and the adjacent solution respectively. The product DK is the methanol permeability (P), which was calculated from the slope of the straight-line plot of methanol concentration vs. permeation time. The measurements were carried out at room temperature of 30 °C.

### Instrumental characterization

The X-ray diffraction (XRD) patterns of the membranes were recorded on "X" Pert Pro diffractometer. The scanning angle was from 1 to 80° with a scanning rate of 2° per minute. The Fourier Transform Infra Red Spectroscopy (FTIR) spectra of SPSEBS and composite membranes were recorded using Perkin Elmer FTIR spectrometer. The differential scanning calorimetry (DSC) analysis of composite membranes was carried out on NETZSCH- Geratebu model DSC 200PC. Measurements were performed between 28 and 300 °C at a heating rate of 10 °C/min in hermetically sealed aluminium pans. Thermal stability of polymer films was examined using NETZSCH-Geratebu GMBH from 27 to 900 °C and at a heating rate of 20 °C/min in nitrogen atmosphere. The surface morphology was studied by scanning electron microscopy (SEM) using a JOEL JSM 6360 microscope. The proton conductivity was determined by AC impedance technique at frequency range of 10 Hz to 40 KHz in the hydrated condition. The conductivity of sample ( $\sigma$ ) was measured using the following formula.

$$\sigma = L/RA$$

Where, L is the thickness of the membrane in cm, A is the area of the membrane in  $cm^2$ , R is the resistance in  $\Omega$  and  $\sigma$  is

conductivity in S/cm. Tensile strength of the membranes was measured using Universal Testing Machine (UTM) (Hounsfield) possessing a load cell of 5 kN, at room temperature. The gauge length and breadth of all membranes were 50 mm and 5 mm, respectively. Tests were conducted with a constant strain rate of 10 mm/min and up to failure of the sample.

### Preparation of membrane electrode assembly (MEA)

#### Diffusion layer preparation

The slurry for the gas diffusion layer was prepared by mixing 70 wt% Vulcan XC – 72, 30 wt% poly tetra fluoroethylene (PTFE) binder, double distilled water and isopropyl alcohol. The resulting black mixture was then ultra sonicated for 15 min. A carbon cloth was then coated with the resultant slurry, and it was sintered in the muffle furnace for 3 h at 350 °C [20].

#### Preparation of the anode and cathode electrodes

The catalyst slurry was prepared by mixing 20% Pt/C with isopropyl alcohol and PTFE binder. The above diffusion layer was coated with the catalyst slurry in order to have 0.125 mg/cm<sup>2</sup> and 0.375 mg/cm<sup>2</sup> for anode and cathode, respectively. It was then dried in a muffle furnace at 350 °C for 3 h. Since the oxygen reduction kinetics is lower at the cathode than the anode, the cathode catalyst loading was thrice than that of the anode [21].

#### Hot pressing

The proton conducting membrane was sandwiched between the anode and cathode by hot pressing at 80 °C for 2 min at an applied pressure of 1.5 ton. The Membrane Electrode Assembly (MEA), thus fabricated, was ready to use in PEMFC membrane fuel [22].

#### MEA Preparation for DMFC

Membrane electrode assembly (MEA) was obtained by sandwiching the SPSEBS/ZrPO<sub>4</sub> composite membrane between the anode and cathode. For DMFC, the electrocatalyst used was 40 wt% Pt:Ru (1:1) on Vulcan XC-72 and 20 wt% Pt on Vulcan XC-72 in the anode (loading 0.5 mg/cm<sup>2</sup>) and cathode (loading 0.5 mg/cm<sup>2</sup>), respectively. The catalyst layer is obtained by mixing the catalyst, isopropyl alcohol deionised water and Nafion solution as binder and coated on the carbon cloth. The electrodes were of 5 cm x 5 cm (area = 25 cm<sup>2</sup>). The MEA was fabricated uniaxially by hot pressing the anode and cathode onto the membrane at 100 °C with a pressure of 150 kg/cm<sup>2</sup> for 3 minutes.

## RESULTS AND DISCUSSION

### IEC, Water and Methanol uptake of composite Membranes

Ion exchange capacity (IEC) provides an indication of the acid groups present in the polymer matrix, which are responsible for the conduction of protons and provides a reliable approximation of the proton conductivity. Water uptake and ion exchange capacity of the membrane plays an important role in conductivity. With increase in water uptake and IEC,

proton conductivity increases due to increase in the mobility of ions in the water phase. The IEC, water and methanol uptake for the composite membrane are given in Figures 1, 2 and 3 respectively. At room temperature, the water uptake and IEC increased with increase in ZrPO<sub>4</sub> content, which may be attributed to the hydrophilic nature of ZrPO<sub>4</sub> particles. Methanol uptake also gradually increased with increase in ZrPO<sub>4</sub> content [23].

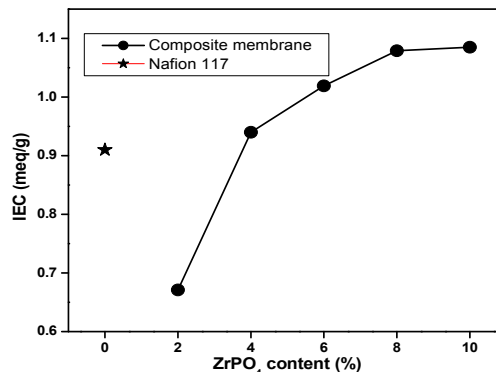


Fig. 1. Ion Exchange Capacity of composite membranes

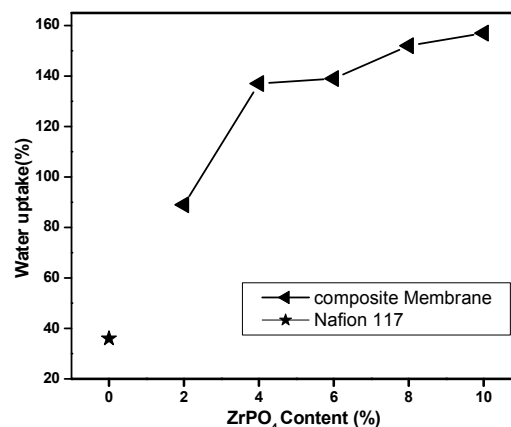


Fig. 2. Water uptakes of composite membranes

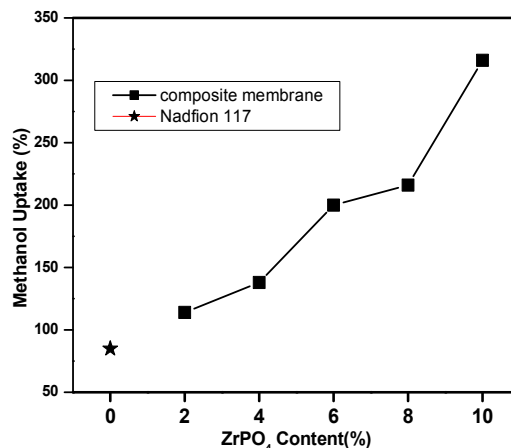


Fig. 3. Methanol uptakes of composite membranes

#### Stability test

Aging test involves the acceleration of the degradation process, thereby indicating the mechanical and chemical stability. The SPSEBS and the composite membranes were introduced into Fenton's reagent (3% hydrogen peroxide with 4 ppm ammonium iron II sulphate hexahydrate) dissolved in 500 ml distilled water at 80 °C. It was found that the membranes did

not exhibit any physical deformation and the membrane was stable for more than 8 hours. The properties measured were ion exchange capacity (IEC), water uptake and proton conductivity. The results obtained after the stability of the membrane were not significantly changed, which meant that the prepared SPSEBS membrane had good mechanical and chemical stability [24].

### Methanol permeability

The methanol permeability of the composite membrane is shown in Fig. 4. The methanol permeability decreased with increasing content of ZrPO<sub>4</sub>. It is known that methanol permeates through hydrophilic ionic channels and that protons are transported by hopping between ionic sites due to hydrogen bonding as well as through ionic channels. Therefore, it could be explained that the methanol permeability decreased as a result of the inorganic particles which blocked the methanol transport while the proton conductivity remained largely unchanged.

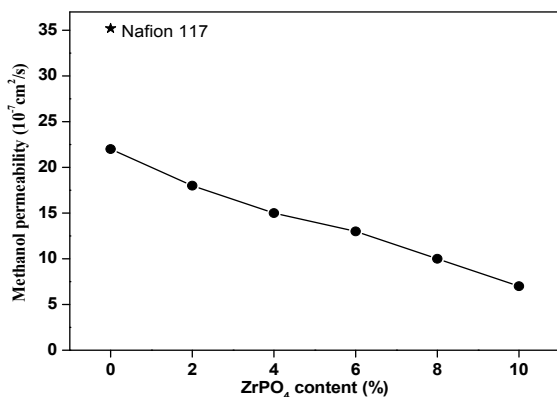


Fig. 4. Methanol permeability of composite membranes

### XRD

Fig. 5 shows the XRD patterns of the ZrPO<sub>4</sub>, SPSEBS and composite membranes (SPSEBS/ZrPO<sub>4</sub>). Three sharp diffraction peaks appeared at  $2\theta = 45, 52,$  and  $74^\circ$  for SPSEBS confirmed the presence of crystallites. The crystal size was computed by Scherrer formula and it was equal to .... In addition the broad band between  $10$  and  $30^\circ$  clarified amorphous portion. Hence SPSEBS was semi crystalline. At 2% loading, the crystallinity decreased dramatically. At higher loading of zirconium phosphate the crystallinity was completely lost. Hence it was confirmed that zirconium phosphate interacted strongly with SPSEBS and prevented formation of tiny crystallites. It was also noted absence of the reflections of ZrPO<sub>4</sub> indicating its high dispersion.

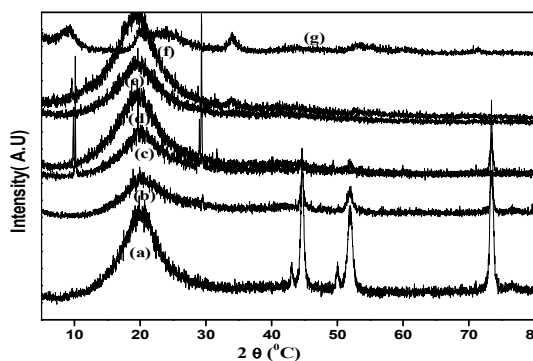


Fig. 5. XRD patterns of SPSEBS and composite membrane (a)SPSEBS (b) Zr 2 (c) Zr 4 (d) Zr 6 (e) Zr 8 (f) Zr10 (g) ZrPO<sub>4</sub>

### FTIR

The FTIR spectra of SPSEBS, ZrPO<sub>4</sub> and their composite membranes are shown in Fig. 6. The intense broad band at  $3410\text{ cm}^{-1}$  was due to -OH stretching vibration of water and sulphonic acid groups. The presence of water was confirmed by its bending vibrations occurring as a shoulder close to  $1640\text{ cm}^{-1}$  to the peak at  $1603\text{ cm}^{-1}$ . The CH<sub>2</sub> vibrations were seen just below  $3000\text{ cm}^{-1}$ . The aromatic ring vibrations were due to the peaks at  $1603$  and  $1445\text{ cm}^{-1}$ . The broad peak just above  $1000\text{ cm}^{-1}$  was due to S=O vibration of sulphonic acid groups. In the spectrum of ZrPO<sub>4</sub> the broadened envelop in the higher energy region was due to OH stretching vibration of water and POH groups. The broadening was attributed to hydrogen bonding. The presence of water was confirmed by its bending vibration close to  $1620\text{ cm}^{-1}$ . The PO<sub>4</sub> vibration occurred just above  $1000\text{ cm}^{-1}$ .

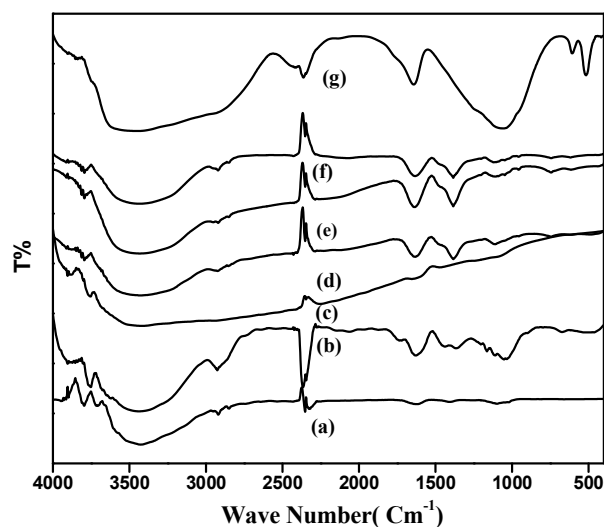


Fig. 6. FTIR spectra of SPSEBS and composite membrane

(a)SPSEBS (b) Zr 2 (c) Zr 4 (d) Zr 6 (e) Zr 8 (f) Zr10 (g) ZrPO<sub>4</sub>

### DSC

Fig. 7 shows the DSC curves of composite membranes and SPSEBS. Thermal transitions of membranes were studied by DSC.

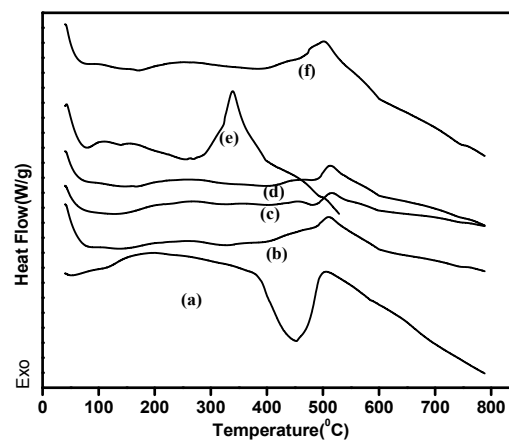


Fig. 7. DSC curve of SPSEBS and composite membrane (a) SPSEBS (b) Zr 2 (c) Zr 4 (d) Zr 6 (e) Zr 8 (f) Zr 10

Ionomer membranes normally show two thermal transitions, one for ionic clusters and the other for polymer backbones. However, highly sulfonated SPSEBS exhibited only a single

glass transition ( $T_g$ ) due to its totally amorphous nature. The DSC curves of SPSEBS showed  $T_g$  around 164 °C. However, there was no evidence in locating the exact transition temperature, since the signal was very weak and broad. The degradation corresponding to the sulphonic acid was same as for 2, 4, and 6% but it differed for 8 and 10% loading of ZrPO<sub>4</sub>.

### TGA

The TGA results of SPSEBS and the composite membranes are illustrated in Fig. 8. In the case of SPSEBS, a three stage decomposition was observed. The first weight loss in SPSEBS was marginal and it occurred between 80 and 150 °C. It was assigned to loss of water. The second loss that occurred between 180 and 260 °C could be due to the decomposition of the sulfonic acid groups from polymer chains. The final weight loss that occurred between 340 and 520 °C was due to degradation of polymer backbone. For all composite membranes similar features of degradation were noted but at slightly lower temperatures. It confirmed the interaction between ZrPO<sub>4</sub> and SPSEBS that decreased the thermal stability.

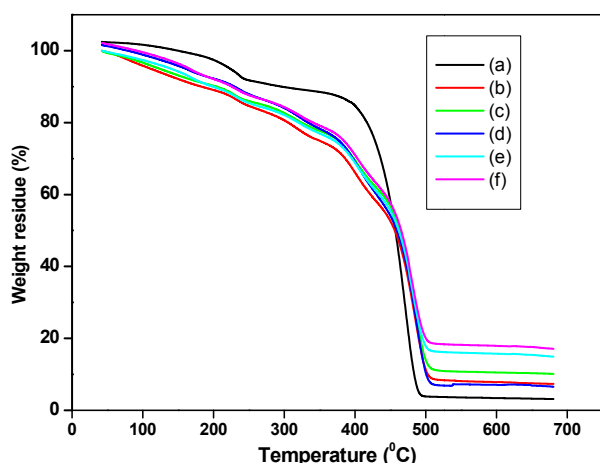


Fig. 8. TGA curve of SPSEBS and composite membrane (a)SPSEBS (b) Zr 2 (c) Zr 4 (d) Zr 6 (e) Zr 8 (f) Zr 10

### SEM

Fig. 9 shows the surface morphology of Zr 2, Zr 6 and Zr10 composite membranes. The nature of pores, level of dispersion and crystal formation were studied by SEM. ZrPO<sub>4</sub> was found to be uniformly distributed over the SPSEBS matrix which facilitated a desirable and efficient matrix for a continuous path way in all directions. Further, the composite membranes were without any voids or pores indicating its suitability as PEM and DMFC.

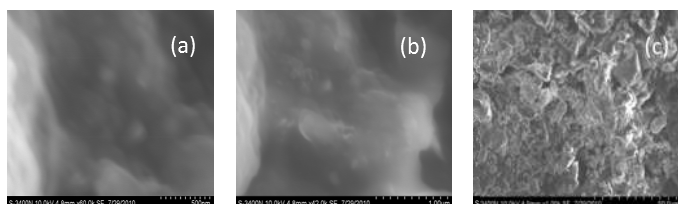


Fig. 9. SEM analysis of (a) Zr 2 (b) Zr 6 (c) Zr 10

### Proton conductivity

The effect of ZrPO<sub>4</sub> loading on the proton conductivity of composite membranes at room temperature is shown in Fig. 10. The increment in proton conductivity was associated with the acidic sites of ZrPO<sub>4</sub> in the presence of water. Hence the proton conductivity increased with increasing content of ZrPO<sub>4</sub> particles.

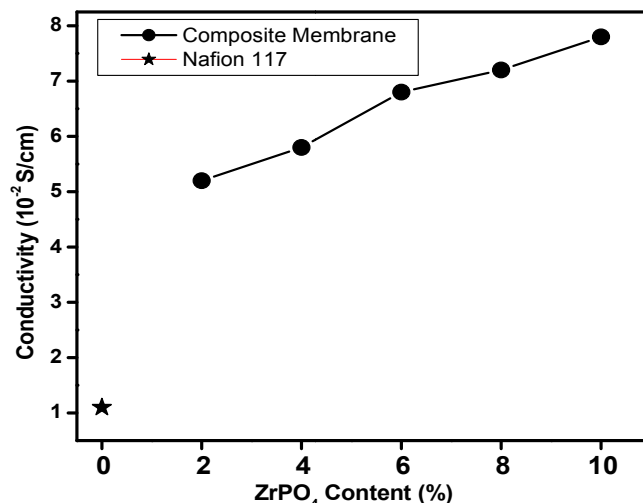


Fig. 10. Proton conductivity of composite membranes

### Mechanical properties

The tensile strength of all the composite membranes is shown in Fig. 11. With the increase in ZrPO<sub>4</sub> content, tensile strength of composite membrane increased. The composite membranes exhibited excellent mechanical properties, indicating that the composite membranes were potential candidates for usage in PEMFC and DMFC.

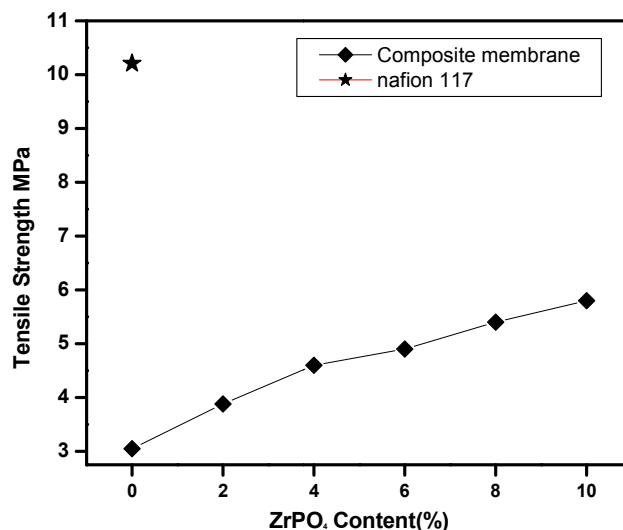


Fig. 11. Tensile strength of composite membranes

### Selectivity ratio

The selectivity ratio of SPSEBS and composite membranes is shown in Fig. 12. The proton conductivity of composite membranes was lower than that of SPSEBS membrane. The virgin SPSEBS membrane and all the composite membranes showed higher selectivity ratio when compared to Nafion 117. Among all the composite membranes, the selectivity ratio of

Zr 10 ( $1.11 \times 10^5 \text{ Ss/cm}^3$ ) showed the highest selectivity. The result suggested that the incorporation of  $\text{ZrPO}_4$  into SPSEBS membranes had greater impact on the reduction of methanol than proton conductivity, and that the composite membranes were attractive for DMFCs. The important criterion for the usage of membranes in DMFC is that, they must possess high proton conductivity and low methanol permeability. The transport of methanol in membrane also requires channels with good connectivity formed by the hydrophilic clusters. The selectivity of SPSEBS/ $\text{ZrPO}_4$  composite membranes, which is based on their conductivities and methanol permeability, is measured at room temperature. The selectivity ranged from 0.28 to  $1.11 \times 10^5 \text{ Ss/cm}^3$ , which was attractive for DMFC performance.

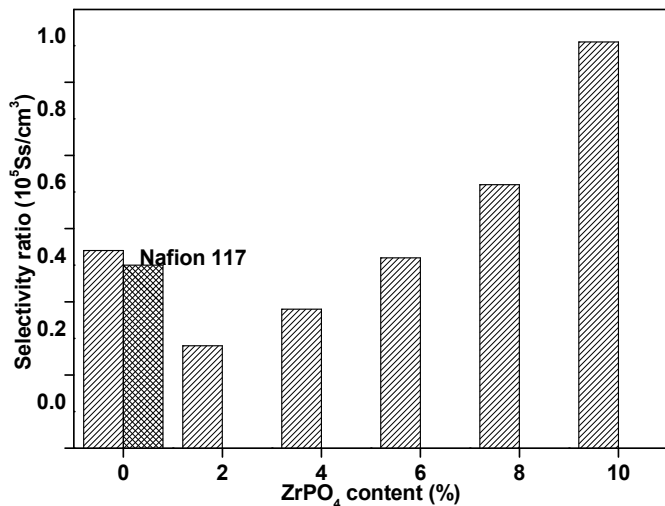


Fig. 12. Selectivity ratios of SPSEBS and composite membranes

**Single cell performance of PEMFC**

To check the functioning of the composite membrane in a real device, the electrochemical performance of the membranes was tested in a PEMFC single cell.

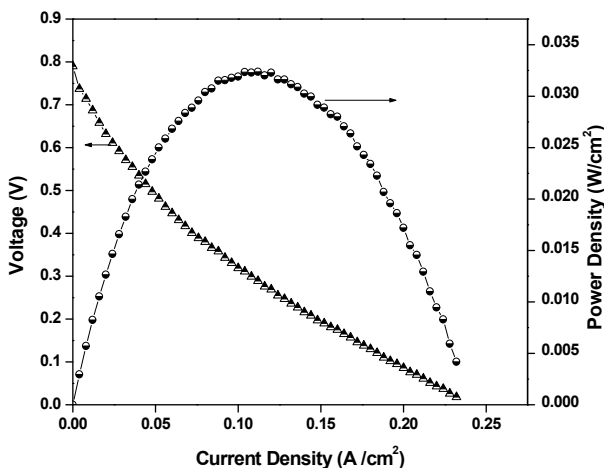


Fig. 13. Polarisation and power density curves of Nafion 117 in PEMFC

was larger than that of Nafion 117 (0.790 V, Figure 13). The OCV value of Zr 2 was 0.770 V which was lesser than that of Nafion 117, whereas the OCV value of Zr 10 was 0.819 V which was higher than that of Nafion 117. In the whole voltage range investigated, the current values of the SPSEBS membrane were always larger than the values obtained with

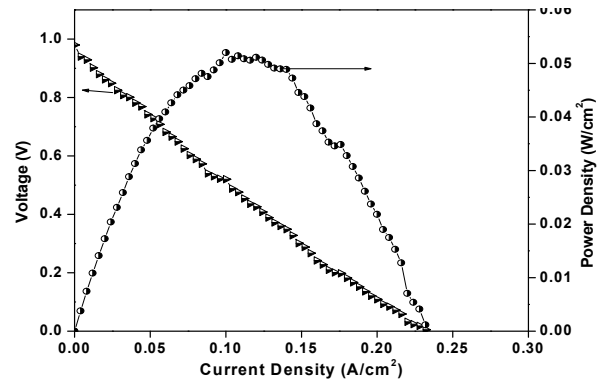


Fig. 14. Polarisation and power density curves of SPSEBS in PEMFC

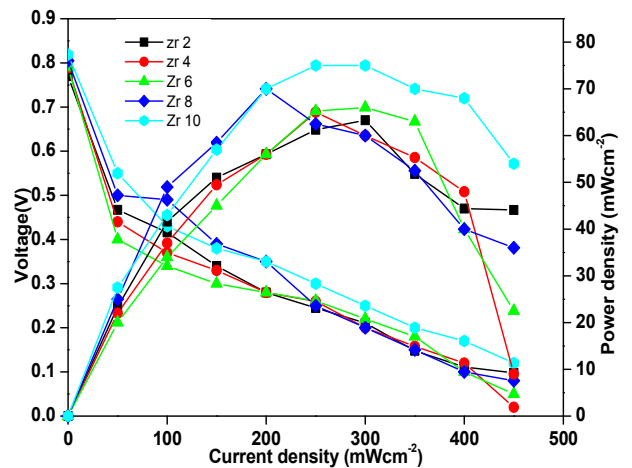


Fig. 15. Polarisation and power density curves of composite membranes in PEMFC

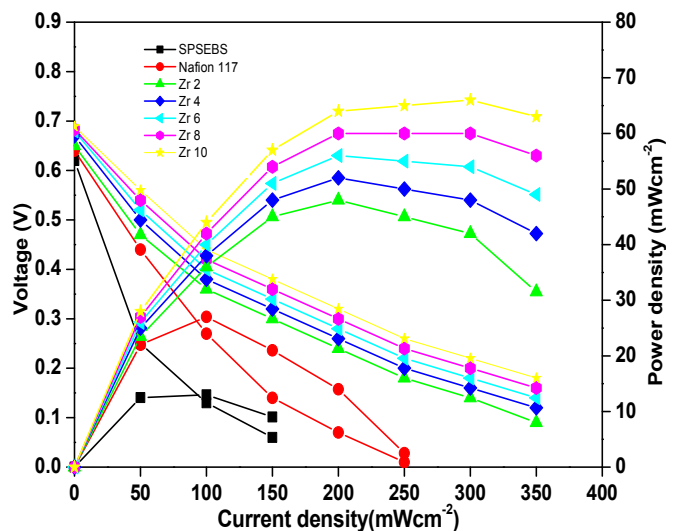


Fig. 16. Polarisation and power density curves of SPSEBS, Nafion 117 and composite membranes in DMFC

Fig.15 shows the polarisation and power density curves for the composite membranes in a PEMFC test at room temperature which was compared with Nafion 117 membrane. The open circuit voltage (OCV) for the SPSEBS (0.980 V, Figure 14)

Nafion 117 membrane. The maximum power density value reached at room temperature with the SPSEBS was  $50 \text{ mWcm}^{-2}$ , whereas the maximum power density of Nafion 117 was  $32 \text{ mWcm}^{-2}$  with the same operating conditions. In the case of composite membrane, the maximum power density values were 63, 65, 66, 70 and  $75 \text{ mWcm}^{-2}$  (Zr 2 to Zr 10) respectively. Power densities of composite membranes were higher than Nafion117. These results indicated that SPSEBS and composite membranes were promising electrolytes for fuel cell [25].

#### DMFC performance of composite membranes

Fig. 16 represents the cell performance based on the composite membranes containing 2 to 10% of zirconium phosphate at room temperature. The open circuit voltage (OCV) for the SPSEBS was 0.62 V. The OCV value of Zr 2 was 0.65 V which was higher than that of Nafion 117. Similarly, the OCV value of Zr 10 was 0.689 V which was also higher than that of Nafion 117. In the whole voltage range investigated, the current values of the composite membrane were larger than the values obtained with Nafion 117 membrane. The maximum power density value reached at room temperature with the SPSEBS was  $13 \text{ mWcm}^{-2}$  whereas the maximum power density of Nafion 117 was  $27 \text{ mWcm}^{-2}$  with the same operating condition. In the case of composite membrane, the maximum power density values were 48, 52, 56, 60 and  $66 \text{ mWcm}^{-2}$  respectively. These results indicated that the performance of the cell based on this composite membrane was comparable to that based on Nafion 117 membrane. This was mainly attributed to the good compatibility of the membrane with the electrode and also its high-dimensional stability [26-28].

#### Conclusions

We successfully fabricated and characterized SPSEBS/ZrPO<sub>4</sub> composite membranes for fuel cells. The proton conductivity of composite membranes was higher than that of Nafion 117. The water and methanol uptake and IEC increased with the increase in the content of ZrPO<sub>4</sub>. The maximum power density and the open circuit voltage were higher than Nafion 117 in PEM fuel cell with the composite membrane. In DMFC also the maximum power density was higher than Nafion 117. Hence the low cost SPSEBS/ZrPO<sub>4</sub> composite membrane is suggested to be very promising for practical application to PEM and direct methanol fuel cells.

#### Acknowledgements

The authors would like to thank the University Grant commission (UGC), INDIA for funding this project.

#### REFERENCES

- S. Schlick, Ionomers: Characterization, Theory and Applications, CRC press, Boca Raton, 1996.
- Q. Chen, K. Schmidt-Rohr, <sup>19</sup>F and <sup>13</sup>C NMR signal assignment and analysis in a perfluorinated ionomer (Nafion) by two-dimensional solid-state NMR, *Macromol.* 37 (2004) 5995-6003.
- A.J. Appleby, F.R. Foulkes, *Fuel Cell Handbook*, Van Nostrand Reinhold, New York, 1989.
- B. Bauer, D.J. Jones, J. Roziere, L. Tchicaya, G. Alberti, M. Casciola, L. Massinelli, A. Peraio, S. Besse, E. Ramunni, *Electrochemical characterisation of sulfonated polyetherketone membranes*. *J. New Mater. Electrochem. Syst.* 3 (2000) 93-98.
- Inan Tuğay Y, Doğan Hacer, Unveren Elif E, Ersoy Eker. Sulfonated PEEK and fluorinated polymer based blends for fuel cell applications: investigation of the effect of type and molecular weight of the fluorinated polymers on the membrane properties. *International Journal of Hydrogen Energy* 2010;35:12038-53.
- G. Alberti, M. Casciola, L. Massinelli, B. Bauer, *Polymeric proton conducting membranes for medium temperature fuel cells (110-160 °C)*, *J. Membr. Sci.* 185 (2001) 73-81.
- F. Lufrano, G. Squadrito, A. Patti, E. Passalacqua, *Sulfonated polysulfone as promising membranes for polymer electrolyte fuel cells*, *J. Appl. Polym. Sci.* 77 (2000) 1250-1256.
- M.J. Coplan, G. Götz, *Heterogeneous sulfonation process for difficultly sulfonatable poly (ether sulfone)* US Patent (1983) 4,413,106.
- R. Nolte, K. Ledjeff, M. Bauer, R. Mülhaupt, *Partially sulfonated poly(arylene ether sulfone)-A versatile proton conducting membrane material for modern energy conversion technologies*, *J. Membr. Sci.* 83 (1993) 211-220.
- T. Lehtinen, G. Sundholm, S. Holmberg, F. Sundholm, P. Björnbom, M. Bursell, *Electrochemical characterization of PVDF-based proton conducting membranes for fuel cells*, *Electrochim. Acta* 43 (1998) 1881-1890.
- F.N. Büchi, B. Gupta, O. Haas, G.G. Scherer, *Study of radiation-grafted FEP-G-polystyrene membranes as polymer electrolytes in fuel cells*, *Electrochim. Acta* 40 (1995) 345-353.
- S. Hietala, M. Koel, E. Skou, M. Elomaa, F. Sundholm, *Thermal stability of styrene grafted and sulfonated proton conducting membranes based on poly(vinylidene fluoride)*, *J. Mater. Chem.* 8 (1998) 1127-1132.
- J.S. Wainright, J.T. Wang, D. Weng, R.F. Savinell, M. Litt, *Acid-doped polybenzimidazoles-a new polymer electrolyte*, *J. Electrochem. Soc.* 142 (1995) L121-L123.
- S.R. Samms, S. Wasmus, R.F. Savinell, *Thermal stability of proton conducting acid doped polybenzimidazole in simulated fuel cell environments*, *J. Electrochem. Soc.* 143 (1996) 1225-1232.
- Q. Guo, P.N. Pintauro, H. Tang, S. O'Connor, *Sulfonated and crosslinked polyphosphazene-based proton-exchange membranes*, *J. Membr. Sci.* 154 (1999) 175-181.
- R. Carter, R. Wycisk, H. Yoo, P.N. Pintauro, *Blended polyphosphazene/polyacrylonitrile membranes for direct methanol fuel cells*. *Electrochem. Solid State Lett.* 5 (2002) A195-A197.
- M. Helen, B. Viswanathan, S.S. Murthy, *Fabrication and properties of hybrid membranes based on salts of heteropolyacid, zirconium phosphate and polyvinyl alcohol*, *J. Power Sources* 163 (2006) 433-439.

18. D. Sangeetha, Sulphonated polystyrene-block-poly(ethylene-ran-butylene)-block polystyrene as polymer electrolytes for proton exchange membrane fuel cell, *Int. J. Plast. Technol.* 8 (2004) 313-321.
19. F. Faverjon, M. Rakib, G. Durand, Electrochemical study of a hydrogen diffusion anode-membrane assembly for membrane electrolysis, *Electrochim. Acta* 51 (2005) 386-394.
20. Ong Ai-Lien, Jung Guo-Bin, Wuc Chia-Ching, Yan Wei-Mon. Single-step fabrication of ABPBI-based GDE and study of its MEA characteristics for high-temperature PEM fuel cells. *International Journal of Hydrogen Energy* 2010;35:7866-73.
21. Bussayajarn Narissara, Ming Han, Hoong Kwan Kian, Stephen Wan Yee Ming, Hwa Chan Siew. Planar air breathing PEMFC with self-humidifying MEA and open cathode geometry design for portable applications. *International Journal of Hydrogen Energy* 2009;34:7761-7.
22. Y.W. Kim, D.K. Lee, K.J. Lee, J.H. Kim, Single-step synthesis of proton conducting poly (vinylidene fluoride) (PVDF) graft copolymer electrolytes, *Eur. Polym. J.* 44 (2008) 932-939.
23. R. Vinodh, A. Ilakkiya, S. Elamathi, D. Sangeetha, A novel anion exchange membrane from polystyrene (ethylene butylene) polystyrene: Synthesis and characterization, *Mater. Sci. Eng., B* 167 (2010) 43-50.
24. M. Helen, B. Viswanathan, S.S. Murthy, Fabrication and properties of hybrid membranes based on salts of heteropolyacid, zirconium phosphate and polyvinyl alcohol, *J. Power Sources* 163 (2006) 433-439.
25. H.-Y. Jung, J.-K. Park, Blend membranes based on sulfonated poly (ether ether ketone) and poly(vinylidene fluoride) for high performance direct methanol fuel cell, *Electrochim. Acta* 52 (2007) 7464-7468.
26. L. J. Hobson, Y. Nakano, H. Ozu, S. Hayase, Targeting improved DMFC performance, *J. Power Sources* [104](#) (2002) 79-84.
27. Devrim Yilser, Erkan Serdar, Bac Nurcan, Eroglu Inci. Preparation and characterization of sulfonated polysulfone/titanium dioxide composite membranes for proton exchange membrane fuel cells. *International Journal of Hydrogen Energy* 2009;34:3467-75.
28. P. Bhavani, D. Sangeetha. Proton exchange membrane based on SPSEBS/PSEBS for fuel cell application. *International journal of current research* 2011: 3: 7; 192-198.

\*\*\*\*\*